Environmental Science & Technology

pubs.acs.org/est

Article

Fe(III) Mineral Encrustation Uncouples Respiration from Reproduction of the Nitrate-Reducing Fe(II)-Oxidizing Bacterium *Acidovorax* sp. BoFeN1

Heping Zhang, Chao Peng,* Zezhen Pan, Guojun Chen, Chenchen Zhang, Lu Lu, Tongxu Liu, Juan Liu, Zimeng Wang, Andreas Kappler, and Hailiang Dong

Cite This: *Environ. Sci. Technol.* 2026, 60, 8507−8516

Read Online

ACCESS | Metrics & More | Article Recommendations | Supporting Information

ABSTRACT: Fe(II) can be oxidized by mixotrophic nitrate-reducing Fe(II)-oxidizing (NRFeOx) bacteria to Fe(III), leading to mineral precipitation. However, the effects of this process on the metabolism and reproductive ability of Fe(II)-oxidizing bacterial cells have not yet been quantified. In this study, we investigated the effects of Fe(II) on the mixotrophic NRFeOx bacteria *Acidovorax* sp. BoFeN1 by performing cell plate counts, chemical analyses, scanning electron microscopy (SEM) imaging, live/dead fluorescence staining, and proteomic analysis. The results showed that nitrate-reducing Fe(II)-oxidizing bacteria *Acidovorax* sp. BoFeN1 undergo a striking physiological state in which respiration persists while cell reproduction collapses after their oxidation of Fe(II). Across 0.1−10 mM Fe(II), colony-forming units dropped by up to 10^3-fold, yet acetate consumption remained largely unaffected, and nitrate reduction was even slightly promoted. SEM-EDS revealed extensive Fe(III) encrustation on cells, while live/dead staining showed intact inner membranes where nitrate reduction occurs. Adding an Fe(III) chelator, citrate, restored reproductive capacity without notable changes in Fe(II) oxidation or nitrate reduction, indicating that it was the products of Fe(II) oxidation, the secondary Fe(III) minerals, that impaired cell reproduction. The phenotypes observed in this study were supported by proteomic analyses, which showed that Fe(II) increased the abundance of proteins involved in nitrate reduction and the respiratory electron transport chain. These findings uncover a mineral encrustation-driven uncoupling between respiration and reproduction, suggest how natural organic ligands may buffer NRFeOx bacterial communities in Fe-rich anoxic environments, and point to cellular-level levers for mitigating denitrification failures and N_2O risks in engineered and natural systems.

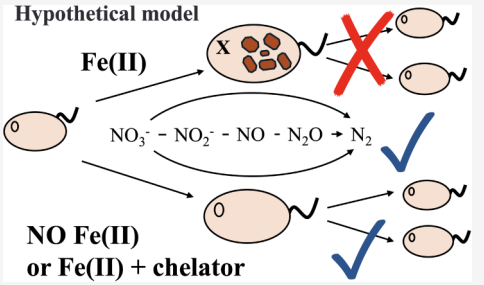

KEYWORDS: *Fe(II), reproductive capacity, iron oxidation, nitrate reduction, metabolism*

INTRODUCTION

In natural environments, bacteria rely on their energy metabolism to maintain cellular functions and survival in competition with other species. However, maintaining cellular functions and survival only is not sufficient, bacteria must also have effective reproductive capacity, not only to expand their populations but even simply to maintain their population size despite cell death.[1]

The metabolism and reproductive capacity of bacteria in natural ecosystems are strongly regulated by diverse environmental factors.[2] Among these factors, iron(Fe) plays an important role. First, iron is an indispensable nutrient for most forms of life, as it is needed for the synthesis of many key enzymes such as cytochromes and Fe−S proteins, which are critical in maintaining energy metabolism and respiratory processes.[3] Second, Fe also serves as an important electron donor and acceptor in energy metabolism.[4] In addition, as the redox potential of the Fe(III)/Fe(II) couple lies between many essential elements,[5] the oxidation and reduction of Fe(II) and Fe(III) are closely linked to the biogeochemical cycles of nitrogen, sulfur, and carbon.[4−6] These include the production and consumption of greenhouse gases, nutrient migration, and ecosystem stability.[7] Third, Fe redox transformations often result in the dissolution and formation of Fe(III) minerals. As these minerals typically have highly reactive surfaces, Fe redox processes are also associated with the fate of many nutrients and pollutants in the environment.[8,9]

In anoxic environments, such as groundwater, soils, and sediments, Fe(II) is abundant[10] and can be oxidized to Fe(III) by anaerobic Fe(II)-oxidizing bacteria.[11] Among these bacteria, mixotrophic nitrate-reducing Fe(II)-oxidizing (NRFeOx) bacteria use NO_3^- as an electron acceptor and oxidize Fe(II) and organic matter. In this process, mixotrophic NRFeOx

Received: November 4, 2025
Revised: February 26, 2026
Accepted: March 2, 2026
Published: March 10, 2026

https://doi.org/10.1021/acs.est.5c15463
Environ. Sci. Technol. 2026, 60, 8507−8516

bacteria utilize organic matter as an electron donor to reduce nitrate (NO_3^-) to intermediates such as nitrite (NO_2^-) inside the cells. In parallel, Fe(II) is oxidized to Fe(III) partly enzymatically but also through a series of chemical reactions with NO_2^- and NO, accompanied by the production of greenhouse gases such as N_2O.[12,13] In one study, it was suggested that most of the Fe(II) (>99%) is oxidized chemically by the reactive N-intermediates produced during the denitrification process (i.e., chemodenitrification),[14] implying that this process is widespread among different nitrate-reducing bacteria,[15] while another recent study has suggested a significantly larger fraction of enzymatic Fe(II) oxidation.[13]

Recent studies have shown that the interaction between NRFeOx bacteria and Fe(II) is bidirectional: these bacteria are capable of oxidizing Fe(II) and reducing NO_3^-, and Fe(II) may also adversely affect NRFeOx bacteria. For example, Fe(II) addition has been shown to significantly alter the community structure of nitrate-reducing bacteria in soil[16] and inhibit nitrate reduction by *Pseudogulbenkiania* sp. strain 2002.[17] Moreover, nitrate-reducing bacteria can alter the expression of nitrite reductase and nitric oxide reductase in response to substrate concentrations.[18,19] These genetic systems are important in regulating the accumulation of toxic intermediates such as NO_2^- and NO.[18,20] However, in the presence of Fe(II), significant NO_2^- accumulation often occurs during laboratory incubations, sometimes reaching millimolar concentrations, even though NO_2^- is simultaneously consumed through reactions with Fe(II).[21,22] Furthermore, electron microscopy studies have shown that upon Fe(II) oxidation, the resulting Fe(III) minerals often precipitate on the cell surface of mixotrophic NRFeOx bacteria, within the periplasmic space, or even inside the cytoplasm,[12,22−24] suggesting potential interference of Fe(II) oxidation with microbial cell division.

Although previous studies have indicated that the metabolism of mixotrophic NRFeOx bacteria responds to the presence of Fe(II) compared to Fe(II)-free conditions,[25] systematic and quantitative investigations of the effects of Fe(II) on the metabolism and cell reproductive capacity of these bacteria are still lacking. In addition, previous studies have suggested that natural organic matter in the environment can act as an Fe(III)-chelator, forming Fe(III)−OM complexes,[26−28] thereby preventing the formation of Fe(III) minerals. However, whether and to what extent such organic chelators can reduce the negative impacts of Fe(II) on mixotrophic NRFeOx bacteria remains unclear.

The objective of this study, therefore, was to quantitatively evaluate the effect of Fe(II) on the metabolism and reproductive capacity of NRFeOx bacteria. We hypothesize that the formation of Fe(III) minerals, as a result of Fe(II) oxidation, inhibits the reproductive capacity of NRFeOx bacteria, but keeping the Fe(III) in solution by organic ligands removes this inhibitory effect. By assessing colony-forming units (CFU) to evaluate reproductive capacity, together with chemical analyses, scanning electron microscopy (SEM) observations, live/dead fluorescence staining, and proteomic analysis, we systematically investigated the effects of Fe(II) on the metabolism and reproductive capacity of the mixotrophic NRFeOx bacterium *Acidovorax* sp. BoFeN1.

MATERIALS AND METHODS

Bacterial Strain and Medium

The bacterial strain *Acidovorax* sp. BoFeN1 is a mixotrophic NRFeOx bacterium originally isolated from sediments of Lake Constance, Germany.[21] The strain was inoculated with 1% (v/v) using a modified anaerobic low-phosphate mineral medium[29] for subculturing. The headspace of the bottle was filled with N_2/CO_2 (90:10, v/v) and closed with airtight butyl stoppers. The composition of the medium included $NaHCO_3$ 1.85 g/L, KH_2PO_4 0.14 g/L, NH_4Cl 0.3 g/L, $MgSO_4{\cdot}7H_2O$ 0.5 g/L, $CaCl_2{\cdot}2H_2O$ 0.1 g/L, NaCl 0.2 g/L, 1 mL/L vitamin solution, SL-10 trace element solution, and selenite−tungstate solution. The pH was adjusted to 7.0 by using HCl. The medium was further amended with 10 mM anoxic sodium nitrate ($NaNO_3$) as the electron acceptor and 5 mM anoxic sodium acetate (CH_3COONa) as the electron donor. Cultures were incubated at 28 °C in the dark.

Microbial Cultivation with Different Fe(II) Concentrations

To investigate the influence of Fe(II) on the reaction kinetics and colony-forming capacity of NRFeOx bacteria, experiments were conducted as a function of the Fe(II) concentration. Five different Fe(II) concentrations were added to the growth medium: 0 (control), and 0.1, 1, 5, and 10 mM $FeCl_2$. Each treatment was inoculated with 1% *Acidovorax* sp. BoFeN1 in triplicate under anoxic conditions. In all experiments, $FeCl_2$ was added to the medium prior to inoculation to minimize mineral precipitation on the cell surfaces at the beginning of the experiments.

Microbial Cultivation with Citrate as an Fe(III) Chelator

To assess whether organic chelators could decrease the effect of Fe(II) on NRFeOx bacteria, 10 mM sodium citrate was added to the treatment with 10 mM $FeCl_2$. A control group with only 10 mM sodium citrate but no $FeCl_2$ was also included to exclude any potential effects of citrate itself on bacterial growth. Each treatment was inoculated at 1% inoculum with three biological replicates and incubated at 28 °C, in the dark, under static and anoxic conditions.

Sampling and Chemical Analysis

During the 6-day incubation, subsamples were collected daily inside an anoxic glovebox (100% N_2, mBraun Unilab Pro) using sterile syringes until Fe(II) concentration reached a steady state. The subsamples were centrifuged to collect the supernatant, which was diluted with ultrapure water and filtered through a 0.22 μm membrane. Aqueous concentrations of NO_3^-, NO_2^-, and acetate were measured with an ion chromatograph (ICS-2100, Thermo Scientific).

To determine the kinetics and extent of Fe(II) oxidation, Fe(II) was quantified using the ferrozine assay.[30] Subsamples were taken daily in an anoxic glovebox (100% N_2) throughout the 6-day incubation. To prevent abiotic oxidation of Fe(II) by nitrite under low pH, samples were diluted using anoxic 40 mM sulfamic acid in 1 M HCl.[31] After 2 h of incubation in the dark, Fe(II) concentration was measured using a mixture of 1 M HCl and 0.1% (w/v) ferrozine solution in ammonium acetate (50% w/v). The resulting purple Fe(II)−ferrozine complex was quantified at 562 nm with a spectrophotometer (Multiskan GO, Thermo Scientific). Standard solutions were prepared from $(NH_4)_2Fe(SO_4)_2{\cdot}6H_2O$. Each biological replicate consisted of three technical replicates (i.e., 3 biological × 3 technical replicates = 9 replicates in total).

For Fe speciation analysis, subsamples were collected in an anoxic glovebox and immediately filtered through 0.22 μm Millex-GP filters inside the glovebox. The filtrate was used to determine the concentrations of aqueous Fe(II) and Fe(III). Total Fe was determined after subsamples were extracted with 6 M HCl at 60 °C for 2 h in the dark. Fe(II) concentrations were measured by using the same ferrozine method applied for the determination of Fe(II) oxidation kinetics. Solid-phase Fe(II) and Fe(III) concentrations were calculated by subtracting the aqueous Fe(II) and Fe(III) concentrations from the total Fe(II) and Fe(III) concentrations measured in the unfiltered subsamples.

https://doi.org/10.1021/acs.est.5c15463
Environ. Sci. Technol. 2026, 60, 8507−8516

To evaluate microbial biomass production under different conditions, total protein was quantified using the Coomassie Brilliant Blue method.[32] Samples were collected right after inoculation (day 0) and at the stationary phase (day 6). Samples were centrifuged (9000 g, 10 min), and the pellets were resuspended in a mixture containing 0.2 M oxalate and 0.1 M $FeC_2H_4(NH_3)_2SO_4$, followed by incubation at 30 °C for 30 min to remove Fe(III).[33] After mineral dissolution, 10 mM trichloroacetic acid (TCA) was added, and samples were incubated on ice for 30 min and then centrifuged again (14000 × g, 15 min). Protein precipitates were dissolved in 500 μL of 0.1 M NaOH, heated in a metal bath at 100 °C, and stained with Coomassie Brilliant Blue dye for 10 min. Absorbance at 595 nm was measured using a spectrophotometer (Multiskan GO, Thermo Scientific). Bovine serum albumin (BSA) was used as a standard. To avoid any interference from mineral precipitates, the same concentrations (10 mM Fe(III)) of synthetic ferrihydrite[34] were added to the standard solutions. The standards were subjected to the same mineral dissolution treatment as the samples, and the added Fe(III) minerals were removed prior to Coomassie staining and absorbance measurement.

Colony-Forming Units (CFU)

Reproductive capacity was assessed by quantifying colony-forming units (CFU) in this study. To quantify viable cell counts (CFU) at different time points, subsamples were taken on days 1, 3, and 6. To prevent potential effects of reactive oxygen species generated from the reaction between Fe(II) and O_2,[35] all sampling and dilutions were performed in an anoxic glovebox (100% N_2) using sterile syringes. Samples were serially diluted in 1× anoxic PBS buffer (NaCl 8 g/L, KCl 0.2 g/L, Na_2HPO_4 1.44 g/L, KH_2PO_4 0.24 g/L, pH 7.4). Dilution ranged from 10^4 to 10^6 to ensure maximum Fe(II) concentrations were below 100 nM. Diluted samples were removed from the glovebox, spread on R2A agar plates (yeast extract 0.5 g/L, peptone 0.5 g/L, casein hydrolysate 0.5 g/L, glucose 0.5 g/L, soluble starch 0.5 g/L, K_2HPO_4 0.3 g/L, $MgSO_4{\cdot}7H_2O$ 0.024 g/L, sodium pyruvate 0.3 g/L, agar 15 g/L, pH 7.2 ± 0.2), and incubated at 28 °C in the dark for about 3 days. Colonies were then counted to calculate the CFU. To verify whether Fe(II) interfered with the CFU determination, $FeCl_2$ was added to Fe(II)-free samples before dilution and plating. Results were comparable to controls without $FeCl_2$, indicating that residual Fe(II) did not significantly affect CFU enumeration (Figure S1, Supporting Information).

Scanning Electron Microscopy (SEM)

To examine the effect of citrate as an Fe(III) chelator on cell encrustation by Fe(III) minerals, SEM was performed for 10 mM $FeCl_2$ treatment at day 6, with or without 10 mM sodium citrate. Cells were harvested by centrifugation (3000 × g, 10 min), washed three times with PBS buffer, and fixed with 2.5% glutaraldehyde at 4 °C. Prior to imaging, fixed cells were rinsed three times (15 min each) with 0.1 M phosphate buffer (pH 7.0). Then cells were fixed with 1% osmium tetroxide for 1−2 h and rinsed again three times with PBS buffer. Samples were then dehydrated in graded ethanol solutions (30, 50, 70, 80, 90, 95%, 15 min each), followed by two treatments with 100% ethanol (20 min each). Subsequently, samples were transferred to a 1:1 ethanol/isoamyl acetate solution for 30 min and to pure isoamyl acetate for overnight incubation at room temperature. After the critical point drying, dried samples were mounted on SEM stubs, fixed with conductive adhesive, and sputter-coated with gold for 60 s. Imaging and elemental analysis were performed with a Zeiss Sigma 300 scanning electron microscope equipped with an Oxford Xplore 30 EDS detector.

Live and Dead Cell Staining

To assess the status of the cell membranes under different incubation conditions, live/dead fluorescence staining was performed. Cultures were harvested on day 6 by centrifugation (5000 g, 15 min), washed twice with 0.85% (w/v) NaCl solution, and resuspended in the same solution. A staining working solution was freshly prepared by mixing 1 μL of NucGreen dye and 2 μL of EthD-III dye with 8 μL of 0.85% NaCl solution (EX3000, Solarbio). For staining, 10 μL of the working solution was added to 1 mL of the cell suspension, and the mixture was gently mixed and incubated at room temperature for 15 min in the dark. After incubation, 10 μL of the stained suspension was mounted on a glass slide, covered with a coverslip, and photographed using an Olympus BX51 fluorescence microscope equipped with a U-MNG2 filter set.

Proteomics

Acidovorax sp. BoFeN1 was cultivated in triplicate in the presence or absence of 10 mM $FeCl_2$. After 6 days of incubation, cells were harvested by centrifugation, immediately frozen in liquid nitrogen, and stored at −80 °C until analysis. Proteomic analysis was performed using a data-independent acquisition-based workflow. Proteins were extracted, digested with trypsin, and the resulting peptides were analyzed using a Vanquish Neo UHPLC system coupled to a timsTOF HT mass spectrometer (Bruker, Germany) operated in DIA mode. Protein identification and quantification were conducted using Spectronaut (version 19) with a false discovery rate of ≤1% at both peptide and protein levels, and protein abundance was calculated using the MaxLFQ algorithm. Differentially expressed proteins were identified based on a fold change >1.2 or <0.83 and $P < 0.05$. Functional annotation and enrichment analyses were performed using GO and KEGG databases. Detailed experimental procedures are provided in the Supporting Information.

RESULTS

Fe(II) Oxidation Rates and Extents

Kinetic analyses showed that the Fe(II) concentration significantly affected the Fe(II) oxidation rate (Figure 1a). With 0.1, 1, 5, and 10 mM $FeCl_2$ added, the oxidation rate increased with the initial Fe(II) concentration (Figure 1a), reaching 0.02 ± 0.01, 0.17 ± 0.02, 0.79 ± 0.02, and 1.54 ± 0.01 mM/day, respectively. Residual Fe(II) concentrations at the end of the reaction were all below 0.36 mM. Despite clear

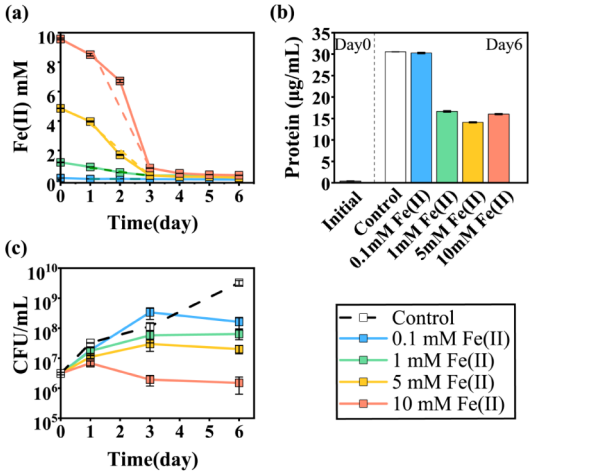

Figure 1. Time-course changes of Fe(II) concentrations, CFU, and protein concentrations during the cultivation of *Acidovorax* sp. BoFeN1 under different initial Fe(II) concentrations: (a) Fe(II) concentrations, (b) protein concentrations (day 6), and (c) colony-forming unit (CFU) counts. "Control" represents the treatment without the addition of $FeCl_2$, while 0.1, 1, 5, and 10 mM Fe(II) correspond to treatments with the respective concentrations of $FeCl_2$. The results showed that the Fe(II) oxidation rate increased with initial Fe(II) concentrations. CFU counts (cell reproductivity) decreased with increasing Fe(II) concentrations, with a maximum reduction of more than 3 orders of magnitude at 10 mM Fe(II), whereas the difference in protein concentration was only about 50%. Error bars represent the standard deviations of three biological replicates.

https://doi.org/10.1021/acs.est.5c15463
Environ. Sci. Technol. 2026, 60, 8507−8516

differences in the Fe(II) oxidation rates among the treatments, the percentage of Fe(II) oxidation within the same cultivation period (i.e., oxidized Fe(II) relative to the initial Fe(II) added) was highly consistent (ranging from 13.3 to 16.3%/day, Figure S2). For instance, under both 5 and 10 mM Fe(II), approximately 50% of Fe(II) was oxidized by day 2, and the extent of oxidation reached equilibrium by days 5−6 (Figure S2).

In contrast, citrate exhibited a minor effect on the Fe(II) oxidation rate (Figure 2a). With 10 mM $FeCl_2$ plus 10 mM sodium citrate, the oxidation rate and final extent were 1.32 ± 0.02 mM/day and 81.83%, respectively, only slightly lower than those without citrate (1.54 ± 0.01 mM/day and 96.78%). Thus, the chelator had a negligible effect on the rate and extent of Fe(II) oxidation.

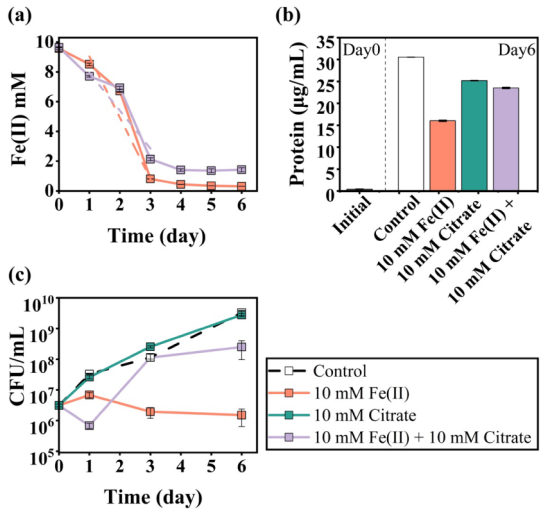

Figure 2. Time-course changes of Fe(II) concentrations, CFU, and protein concentrations during the cultivation of *Acidovorax* sp. BoFeN1 with the addition of citrate as an Fe(III) chelator: (a) Fe(II) concentrations, (b) protein concentrations (day 6), and (c) colony-forming unit (CFU) counts. "Control" represents the treatment without the addition of $FeCl_2$ and citrate, "10 mM Citrate" represents the treatment with 10 mM sodium citrate only, "10 mM Fe(II)" represents the treatment with 10 mM $FeCl_2$ only, and "10 mM Fe(II) + 10 mM Citrate" represents the treatment with both 10 mM $FeCl_2$ and 10 mM sodium citrate. The results show that sodium citrate had little effect on the Fe(II) oxidation rate but greatly enhanced CFU counts. Error bars represent the standard deviations of three biological replicates.

Biomass Production

To evaluate the effect of Fe(II) on the production of total biomass, we compared protein concentrations right after inoculation and at the end of Fe(II) oxidation (day 6) (Figure 1b). The results showed that the concentrations of total protein did not differ significantly among different treatments, ranging from 14 to 31 μg/mL, much smaller than the difference in CFU. The control without Fe(II) and the treatment with 0.1 mM $FeCl_2$ had the highest protein concentrations on day 6 (30.55 ± 0.01 and 30.38 ± 0.19 μg/mL, respectively). With increasing Fe(II), protein production decreased; in the 1, 5, and 10 mM $FeCl_2$ treatments, there were 16.66 ± 0.33, 14.43 ± 0.18, and 16.02 ± 0.10 μg/mL total protein on day 6, respectively (Figure 1b). Similarly, in the treatment with 10 mM $FeCl_2$ plus 10 mM sodium citrate, the protein concentration on day 6 was 23.53 ± 0.13 μg/mL, which was about 1.5-fold higher than the same Fe(II) treatment without chelator, and close to the level in the citrate-only control (25.18 ± 0.02 μg/mL) meaning that citrate did not strongly promote the growth of the bacteria.

Colony-Forming Units (CFU)

To assess how Fe(II) oxidation affects the reproducibility of mixotrophic NRFeOx bacteria, we compared CFU counts of *Acidovorax* sp. BoFeN1 right after inoculation (day 0), during early oxidation (day 1), middle oxidation (day 3), and when Fe(II) oxidation was finished (day 6) under different Fe(II) concentrations, with or without citrate.

The results showed that Fe(II) oxidation markedly decreased the reproductive capacity of this bacterium (Figure 1c). Compared to the Fe(II)-free control, cultures with $FeCl_2$ showed similar CFU on day 1 (both in the 10^6−10^7 range). However, as incubation proceeded, the gap increased on days 3 and 6, with CFU in $FeCl_2$ treatments decreasing by nearly 2−3 orders of magnitude. The extent of inhibition by Fe(II) oxidation was inversely proportional to the initial concentration of Fe(II) (Figure 1c). By day 6, in the samples with 0.1, 1, 5, and 10 mM Fe(II), the CFU counts were about 20.2-, 51.1-, 161.5-, and 1699-fold lower than the Fe(II)-free control, respectively.

To test whether an Fe(III) chelator could decrease Fe(II)-induced inhibition of cell reproductive capacity by dissolving Fe(III) minerals, we compared the CFU in the 10 mM $FeCl_2$ treatment with and without 10 mM sodium citrate. The results showed that the addition of citrate largely restored the reproductivity of the cells (Figure 2c), similar to the effect of lowering the Fe(II) concentration.

Consumption of Nitrate and Acetate

To determine whether the lower CFU and protein content in Fe(II) treatments resulted from a lack of respiration, we measured changes in nitrate, nitrite, and acetate concentrations over time. The results showed that despite the lower CFU counts and protein concentrations in the $FeCl_2$ treatments than the control, Fe(II) neither inhibited nitrate reduction nor acetate oxidation. In fact, nitrate reduction was significantly promoted in the treatments with $FeCl_2$ but its onset was slightly delayed (Figure 3a). The rate and extent of nitrate reduction were positively proportional to the Fe(II) concentration (Figure 3a). Treatments with 10 mM $FeCl_2$ showed both higher nitrate reduction rates (6.29 ± 0.05 mM/day and 89.74%) than the Fe(II)-free control (4.21 ± 0.06 mM/day and 47.58%) (Table S1). Meanwhile, nitrite accumulation also showed a clear correlation with the Fe(II) concentration (Figure S3). In the control and 0.1−1 mM $FeCl_2$ treatments, there was no nitrite accumulation. In those treatments with higher amounts of Fe(II) oxidation (either 5 or 10 mM $FeCl_2$), small amounts of nitrite accumulated, suggesting that high levels of Fe(II) may have imposed pressure on cells to further reduce nitrite. However, amendment with citrate eliminated nitrite accumulation (Figure S3).

Similar to the nitrate reduction curves, compared to the control without Fe(II), the treatments with $FeCl_2$ showed a slightly delayed onset of acetate oxidation, but their rate and final extent did not decrease. The acetate consumption rate was 3.60 ± 0.03 mM/day in treatments with 10 mM $FeCl_2$, compared to 3.39 ± 0.01 mM/day in the Fe(II)-free control (Table S1). In all treatments, acetate was completely

https://doi.org/10.1021/acs.est.5c15463
Environ. Sci. Technol. 2026, 60, 8507−8516

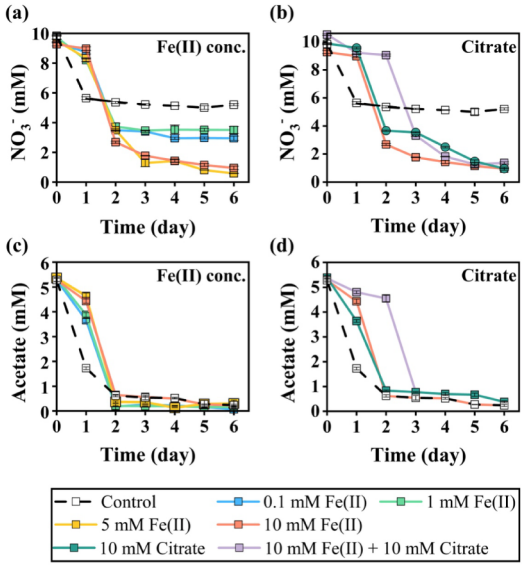

Figure 3. Temporal changes in nitrate (a, b) and acetate (c, d) concentrations under different Fe(II) concentrations (a, c) and with or without citrate (b, d). The results show that the addition of Fe(II) and sodium citrate both promoted nitrate reduction by *Acidovorax* sp. BoFeN1. Although the combined addition of 10 mM $FeCl_2$ and 10 mM sodium citrate delayed the onset of nitrate reduction and acetate oxidation, the final extent and overall rates were comparable to those in the 10 mM Fe(II) treatment. Error bars represent the standard deviations of three biological replicates.

consumed after incubation for approximately 2−3 days (Figure 3c).

Addition of 10 mM citrate had a negligible effect on nitrate reduction and acetate consumption rates but delayed the onset of both processes (Figure 3b,d). Overall, compared to the Fe(II)-free control, high Fe(II) concentration strongly suppressed the reproductive capacity of *Acidovorax* sp. BoFeN1 but did not inhibit acetate oxidation and nitrate reduction.

Visual Observation of Cell−Mineral Interactions

To test whether the higher cell reproducibility in the treatment with citrate was a result of decreased cell encrustation by Fe(III) minerals, we compared cell morphology and cell−mineral interactions/associations using SEM-EDS for cultures grown for 6 days with 10 mM $FeCl_2$ only and 10 mM $FeCl_2$ plus sodium citrate. In the treatment with 10 mM $FeCl_2$ only, many mineral-like structures were observed on cell surfaces (Figure 4d). EDS results revealed that those mineral-like structures were Fe-rich, suggesting that they are Fe(III) minerals (Figure 4e, f). In contrast, cells from the $FeCl_2$ plus citrate treatment had smoother surfaces without such mineral-like structures, and EDS detected no obvious Fe signal (Figure 4a, b, and c). These results suggest that the decreased cell reproductive capacity is indeed a result from Fe(III) mineral precipitation caused by Fe(II) oxidation, rather than from Fe(II) ions.

Consistent with SEM observations, not only did the culture media differ in color, but cell pellets on day 6 also differed visually. In the treatment without $FeCl_2$ and the one with $FeCl_2$ plus citrate, cell pellets were white- and yellow-colored, respectively (Figure S4). This suggests that they were mostly pure biomass. In contrast, pellets in the 10 mM $FeCl_2$ treatment were brown-colored, indicating substantial iron mineral deposition (Figure S4).

Live and Dead Cell Staining

To examine the status of cell membranes under Fe(II) conditions, live/dead fluorescence staining was performed and visualized by using a fluorescence microscope. In the Fe(II)-free control, nearly all cells showed green fluorescence (98.8 ± 0.5% green), indicating intact inner cell membranes (Figure 5a). In contrast, compared to the Fe(II)-free control, cultures incubated with 10 mM $FeCl_2$ showed a much higher proportion of red-fluorescent cells (39.1 ± 1.5% red),

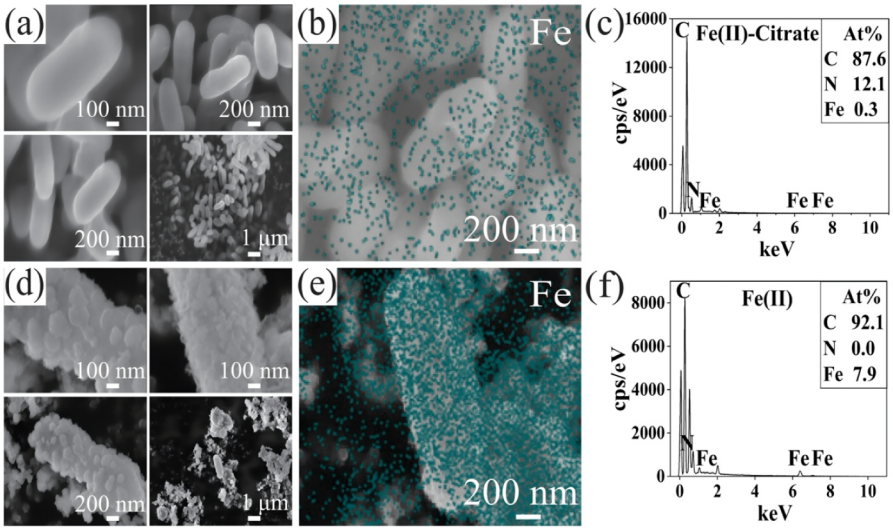

Figure 4. Scanning electron microscopy (SEM) and energy-dispersive spectroscopy (EDS) analyses of *Acidovorax* sp. BoFeN1 cells after 6 days of cultivation under different conditions. SEM images of cells grown in the treatment containing both 10 mM $FeCl_2$ and 10 mM sodium citrate (a), and in the treatment containing 10 mM $FeCl_2$ only (d). SEM image and corresponding EDS Fe elemental map for the 10 mM $FeCl_2$ + 10 mM citrate treatment (b), and for the 10 mM $FeCl_2$-only treatment (e). The EDS spectra for the 10 mM $FeCl_2$ + 10 mM citrate and 10 mM $FeCl_2$-only treatments, respectively (c, f). The results demonstrate that no obvious Fe mineral encrustation was observed on the cell surfaces in the presence of citrate, confirming that citrate decreased cell encrustation and, thereby, supported higher CFU abundance.

https://doi.org/10.1021/acs.est.5c15463
Environ. Sci. Technol. 2026, 60, 8507−8516

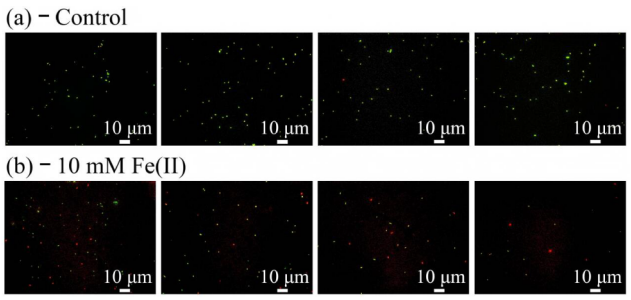

Figure 5. Live/dead fluorescence staining of mixotrophic NRFeOx bacteria under different incubation conditions: (a) Fe(II)-free control and (b) 10 mM Fe(II). Green fluorescence indicates cells with intact membranes, whereas red fluorescence indicates cells with compromised membrane integrity. Images are representative fields of view from different cultures.

indicative of compromised membrane integrity (Figure 5b). Notably, the differences in live and dead cell proportions among the treatments were substantially smaller than those observed in the CFU counts.

Fe(II) and Fe(III) Speciation

To investigate the initial speciation of Fe(II) and Fe(III) generated by Fe(II) oxidation in the 10 mM $FeCl_2$ and Fe(II) plus citrate treatments, the concentrations of Fe(II) and Fe(III) in the aqueous and solid phases were quantified after inoculation and once the reaction reached equilibrium. The results showed that in the $FeCl_2$ plus citrate treatments, nearly all Fe(II) was present in the aqueous phase on day 0. After the Fe(II) oxidation reaction reached equilibrium, the Fe(III) produced also remained mainly in the aqueous phase. In contrast, in the treatment without citrate, nearly all Fe(III) was detected in the solid phase after the Fe(II) oxidation reaction reached equilibrium (Figure 6).

Proteomics

To provide molecular evidence for the observed phenotypes, we compared the proteomes of cells grown in parallel cultures with and without 10 mM $FeCl_2$. Comparative proteomic analysis revealed pronounced changes in protein abundance

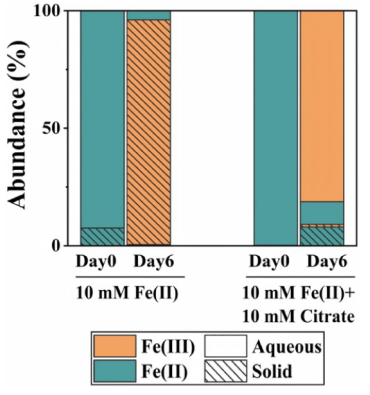

Figure 6. Concentrations of Fe(II) and Fe(III) in the aqueous and solid phases immediately after inoculation and after 6 days of incubation. "10 mM Fe(II)" represents the treatment with 10 mM $FeCl_2$ only, and "10 mM Fe(II) + 10 mM Citrate" represents the treatment with both 10 mM $FeCl_2$ and 10 mM sodium citrate. Fe speciation is expressed as the relative fraction of total Fe partitioned between dissolved and precipitated phases.

under Fe(II) conditions (Tables 1 and 2). The abundance of a set of proteins involved in nitrogen respiration and electron transfer increased, including nitrite reductase (NarI and NarV) and several cytochrome proteins associated with the respiratory electron transport chain (Table 1). In contrast, downregulation was also observed for multiple protein groups under Fe(II) conditions (Table 2). In addition to proteins associated with iron acquisition and transport, proteins linked to cellular growth, carbon storage, and reproductive capacity were also downregulated, such as a phasin family protein and Type I methionyl aminopeptidase (Map). Several proteins involved in cell envelope functions and efflux systems, such as TolC family proteins and RND-type transporter periplasmic adaptor proteins, also decreased.

DISCUSSION

Mechanistic Insights into Fe(II)-Induced Uncoupled Respiratory and Reproductive Capacities

Although Fe(II) oxidation by mixotrophic NRFeOx bacteria has been studied for a long time[21,22,36−39] and has been proposed for potential applications in pollutant migration control and environmental engineering,[40] this study is the first to quantitatively evaluate the effect of Fe(II) on the metabolism and reproductive capacity of the mixotrophic NRFeOx bacteria. Our results demonstrate that the addition of Fe(II) significantly inhibited the reproducibility of mixotrophic NRFeOx bacteria, with a maximum decline of up to about 2.2 × 10^3-fold with 10 mM $FeCl_2$. The inhibition increased with the Fe(II) concentration, and the inhibitory effect of Fe(II) was even evident when the Fe(II) concentration was only 0.1 mM (Figure 1).

However, interestingly, while Fe(II) strongly reduced the bacterial reproductive capacity, it did not strongly suppress the respiration processes (nitrate reduction and acetate oxidation) and protein synthesis (Figure 1b). Consistently, proteomic analyses provided molecular-level support for these physiological observations. In particular, proteins related to nitrate reduction and the respiratory electron transport chain were enriched under $FeCl_2$ conditions, indicating that the core metabolic and respiratory machinery remained active despite a strongly reduced reproductive capacity (Table 1). This result is also consistent with previous reports showing that cells encrusted with Fe(III) minerals could still assimilate acetate,[41] and that *Azospira suillum* strain PS maintained Fe(II) oxidation, nitrate reduction, and acetate consumption even when cell growth was inhibited by chloramphenicol.[15]

Consistent with these observations, live/dead fluorescence staining, which primarily reflects cell inner membrane integrity, showed that most cells remained inner-membrane-intact even under Fe(II) conditions, despite a higher proportion of membrane-compromised cells in the $FeCl_2$ treatment compared to the Fe(II)-free control (Figure 5). This result supported the observed nitrate reduction kinetics in this study (Figure 3), as the key steps of nitrate respiration are associated with membrane-bound enzymatic processes.[2] Meanwhile, this preservation of membrane integrity was also in line with previous transmission electron microscopy (TEM) observations showing that iron minerals formed during Fe(II) oxidation can be distributed both extracellularly and within the periplasm or cell envelope,[23] without disrupting the cytoplasmic membrane of all the cells.

https://doi.org/10.1021/acs.est.5c15463
Environ. Sci. Technol. 2026, 60, 8507−8516

Table 1. Selection of Proteins of Interest with Significantly Higher Abundance in Fe(II) Compared to the Fe(II)-Free Control[a]

			Fe(II) vs Control	
Protein IDs	Description	KO names	log2 FC	adj. p value
Nitrogen respiration				
RDD94225.1	Respiratory nitrate reductase	narI, narV	2.53	2.2×10^{-05}
RDD94224.1	Nitrate reductase molybdenum cofactor assembly chaperone	narJ, narW	1.62	4.8×10^{-03}
RDD91936.1	Heme d1 biosynthesis radical SAM protein NirJ	nirJ	1.53	1.7×10^{-04}
RDD92758.1	Crp/Fnr family transcriptional regulator	dnr	3.51	4.1×10^{-03}
ETC & redox maturation				
WP_236637163.1	FAD:protein FMN transferase	apbE	3.79	4.2×10^{-04}
RDD93034.1	FAD:protein FMN transferase	apbE	2.03	3.6×10^{-02}
RDD91307.1	FAD:protein FMN transferase	apbE	1.14	1.3×10^{-02}
RDD91385.1	Cytochrome C′	CYC	4.30	1.7×10^{-04}
RDD95368.1	Cytochrome c4		4.11	8.6×10^{-05}
RDD92696.1	Cytochrome c oxidase assembly protein	COX11, ctaG	13.32	1.2×10^{-03}
Export/secretion/envelope logistics				
RDD95313.1	Twin-arginine translocase subunit TatC	tatC	9.23	4.8×10^{-03}
RDD94154.1	Outer membrane lipoprotein carrier protein LolA	lolA	4.40	1.7×10^{-04}
Envelope remodeling				
RDD92673.1	Phosphoethanolamine−lipid A transferase	eptA, pmrC	5.43	1.2×10^{-04}
RDD94600.1	Lytic transglycosylase domain-containing protein	slt	2.36	1.7×10^{-04}
RDD94322.1	Lytic transglycosylase domain-containing protein	slt	9.66	4.0×10^{-04}
Ion/metal homeostasis and detox				
RDD91239.1	ZIP family metal transporter	zipB	10.02	1.8×10^{-03}
RDD92801.1	Copper chaperone pcu(A)C	pccA	5.01	1.3×10^{-03}
RDD95055.1	Fluoride efflux transporter crcb	crcB, FEX	10.60	4.2×10^{-02}
Genome maintenance				
RDD95844.1	DNA ligase	lig	3.79	1.2×10^{-04}
RDD95768.1	Helix−hairpin−helix domain-containing protein	comEA	4.04	1.2×10^{-03}
Stress survival and programmed cellular responses				
RDD92444.1	Putative toxin−antitoxin system toxin component		10.39	2.7×10^{-03}

[a]For each comparison: "log2 FC" is the log 2 fold change between Fe(II) and the condition of interest, whilst "adj. p value" represents p values adjusted for multiple testing using the Benjamini−Hochberg false discovery rate. Proteins are grouped broadly into functional groups.

Table 2. Selection of Proteins of Interest with Significantly Lower Abundance in $FeCl_2$ Treatments Compared to the Fe(II)-Free Control[a]

			Fe(II) vs Control	
Protein IDs	Description	KO names	log2 FC	adj. p value
Iron acquisition and transport				
RDD95141.1	Tonb-dependent siderophore receptor	fiu	−5.57	1.8×10^{-04}
RDD91271.1	Tonb-dependent receptor	fiu	−5.42	2.2×10^{-05}
RDD91272.1	Energy transducer tonb	tonB	−1.63	2.7×10^{-03}
RDD92485.1	Fe(3+) ABC transporter substrate-binding protein	afuA, fbpA	−4.33	7.5×10^{-03}
RDD91441.1	Iron ABC transporter permease	afuB, fbpB	−1.72	1.4×10^{-04}
RDD92174.1	ABC transporter ATP-binding protein	afuC, fbpC	−1.20	3.8×10^{-04}
RDD91865.1	Ferrous iron transport protein B	feoB	−4.57	5.6×10^{-04}
Denitrification terminal				
RDD93036.1	Nitrous-oxide reductase	nosZ	−1.13	2.5×10^{-02}
Growth/storage/reproductive capacity				
RDD95029.1	Phasin family protein		−1.04	6.7×10^{-04}
RDD91915.1	Pyruvate kinase	PK, pyk	−1.08	1.9×10^{-04}
RDD91731.1	Type I methionyl aminopeptidase	map	−2.42	6.6×10^{-04}
Envelope/interface/efflux				
WP024815514.1	Tolc family protein		−4.61	5.1×10^{-04}
RDD94894.1	Tolc family protein		−1.13	8.5×10^{-04}
RDD94862.1	Cusa/czca family heavy metal efflux RND transporter		−2.61	1.1×10^{-03}
RDD94932.1	Efflux RND transporter periplasmic adaptor subunit	acrA, mexA, adeI, smeD, mtrC, cmeA	−2.58	1.6×10^{-03}

[a]For each comparison: "log2 FC" is the log 2 fold change between Fe(II) and the condition of interest, whilst "adj. p value" represents p values adjusted for multiple testing using the Benjamini−Hochberg false discovery rate. Proteins are grouped broadly into functional groups.

https://doi.org/10.1021/acs.est.5c15463
Environ. Sci. Technol. 2026, 60, 8507−8516

Although an intact inner cell membrane can sustain metabolic activity, forming colonies requires many additional cellular processes.[2] As the produced Fe(III) minerals were shown to precipitate in the periplasm[23] and outer membrane on the cells (Figure 4), they could disrupt the normal structure of the cell envelope, thereby preventing cell division while leaving intracellular catalyzing enzymes still functional to carry out nitrate reduction and acetate oxidation. Although nitrite is generally considered toxic to many microorganisms,[42] nitrite accumulation was probably also not the primary cause of the reduced reproduction capacity observed under Fe(II) conditions, as the strain grew well using nitrite as the electron acceptor (Figure S5).

Microbial Persistence in Fe(II)-Containing Environments

In this study, even after the oxidation of 10 mM Fe(II), there were still more than $1.50 \times 10^6 \pm 6.77 \times 10^5$ CFU/mL of bacterial cells remaining capable of division and formation of colonies (Figure 1c). This indicates that Fe(II) did not kill all of the NRFeOx bacteria. Repeated subculture experiments further confirmed these observations. When cells previously grown in 10 mM $FeCl_2$ were transferred into fresh medium containing the same $FeCl_2$ concentration, nitrate reduction and Fe(II) oxidation reached rates and extents comparable to those observed during the first incubation under $FeCl_2$ conditions (Figure S6). CFU numbers measured at the end of the subincubation were also comparable to those observed during the first $FeCl_2$ incubation. Similar results were obtained when cells had been cultivated for a third time under $FeCl_2$ conditions.

In fact, NRFeOx bacteria were also frequently detected in certain groundwater systems where dissolved Fe(II) concentrations in natural environments typically range from micromolar to millimolar levels, and can reach values as high as 12 mM.[43,44] In addition, from a geochemical perspective, nitrate-reducing bacteria generally occupy the zones between oxic layers and Fe(III)-reducing zones, meaning that Fe(II) produced during Fe(III) reduction can diffuse into their active niches.[45]

This observation suggests that NRFeOx bacteria may also have a certain extent of resistance to Fe(II). Such resistance may come from several aspects. For example, natural organic matter (NOM) in the environment could also form dissolved Fe(III)−organic complexes.[46,47] This hypothesis is supported by the results of this study: the CFU counts in Fe(II) plus citrate treatments were more than 166-fold higher than in Fe(II)-only treatments, despite the fact that nearly complete Fe(II) oxidation still occurred. Interestingly, after the oxidation of 10 mM Fe(II) together with citrate, approximately 0.11 mM Fe(III) was found in the mineral phase at the end of the reaction (Figure 6), and the extent of CFU reduction under this condition was comparable to that observed upon direct addition of 0.1 mM $FeCl_2$ (Figures 1 and 2). Beyond chelation, other processes may also reduce the Fe(II) oxidation-induced inhibition. These include the extracellular Fe(III) minerals which may function as nucleation sites for secondary minerals,[48] effects of strongly sorbing substances (e.g., citrate and phosphate) on mineral and bacterial surface charge,[49] and at the cellular level, the production of metal efflux proteins or redox-potential-regulating enzymes.[15] Another possibility is that the self-regulation of nitrate reduction capacity by some bacterial cells may also serve as a mechanism by which NRFeOx strains counteract the inhibitory effects of Fe(II) on their growth, as suggested by our proteomic results showing the regulation of nitrate respiration-related proteins under Fe(II) conditions (Tables 1 and 2). This speculation is also supported by observations from different researchers. The same strain, when incubated under different conditions (e.g., with or without organic electron donors),[17,50−52] exhibited divergent behaviors, with some cultures carrying out Fe(II) oxidation normally, whereas others did not. Variation in resistance to Fe(II) among different bacteria may also explain why Fe(II) addition significantly changed soil microbial community structure in previous studies.[16] Thus, when evaluating the inhibitory impact of Fe(II) oxidation on NRFeOx bacteria in natural systems, factors such as NOM (chelators), extracellular Fe(III) minerals, microbial metal efflux capacity, and regulation of reductase activity should be considered as key determinants enabling NRFeOx bacteria to maintain reproductive activity together with Fe(II).

Conclusions and Environmental Implications

The result of this study showed not only that nitrate-dependent Fe(II) oxidation is an important biogeochemical process but also that the resulting Fe(III) mineral could markedly reduce the reproductive ability of NRFeOx bacteria by up to 3 orders of magnitude. Nevertheless, the results also showed that even when bacterial cell reproduction was suppressed, bacterial cells remained metabolically active in terms of nitrate reduction and acetate consumption, supported by higher abundances of proteins involved in nitrogen respiration and respiratory electron transport in these cells. Moreover, our results showed that the inhibitory effect of Fe(II) was caused by the formation of Fe(III) minerals rather than by Fe(II) oxidation itself as Fe(III) chelators strongly decreased the inhibition of bacterial reproduction. These findings also imply that Fe(III) chelators in the environment may similarly protect NRFeOx bacteria from the Fe(II)-induced inhibition effect. Overall, beyond advancing the mechanistic understanding of microbial physiology, this work also provides important implications for agriculture (e.g., nitrogen use efficiency in paddy fields), biogeochemistry (e.g., iron−nitrogen coupled elemental cycles), and wastewater treatment processes that rely on denitrification (e.g., anoxic bioreactors), offering insights into how Fe(II) could be used to optimize the performance of these systems.

■ ASSOCIATED CONTENT

Supporting Information

The Supporting Information is available free of charge at https://pubs.acs.org/doi/10.1021/acs.est.5c15463.

Proteins with significantly higher or lower abundance in the $FeCl_2$ treatment relative to the Fe(II)-free control (XLSX)

Detailed methods for proteomic analysis; additional figures showing control experiments for colony-forming unit (CFU) determination, Fe(II) oxidation percentage at different initial Fe(II) concentrations, and nitrite accumulation during incubation; photographs showing Fe(III) mineral formation under different conditions; metabolic activity and CFU results in cultures supplied with nitrite and acetate; and metabolic activity and CFU of *Acidovorax* sp. BoFeN1 during the second and third transfers under 10 mM $FeCl_2$ conditions; the mass spectrometry proteomics data have been deposited with the ProteomeXchange Consortium via the PRIDE

https://doi.org/10.1021/acs.est.5c15463
Environ. Sci. Technol. 2026, 60, 8507−8516

partner repository under the data set identifier PXD072688 (PDF)

AUTHOR INFORMATION

Corresponding Author

Chao Peng − *Key Laboratory of Southwest China Wildlife Resources Conservation, College of Life Sciences, China West Normal University, Nanchong 637000, China;* orcid.org/0000-0003-3433-4319; Email: chpeng89@cwnu.edu.cn

Authors

Heping Zhang − *Key Laboratory of Southwest China Wildlife Resources Conservation, College of Life Sciences, China West Normal University, Nanchong 637000, China*

Zezhen Pan − *Department of Environmental Science and Engineering, Fudan University, Shanghai 200438, China;* orcid.org/0000-0003-1712-3149

Guojun Chen − *Institute of Eco-Environmental and Soil Sciences, Guangdong Academy of Sciences, Guangzhou 510650, China;* orcid.org/0000-0003-3081-629X

Chenchen Zhang − *Key Laboratory of Southwest China Wildlife Resources Conservation, College of Life Sciences, China West Normal University, Nanchong 637000, China*

Lu Lu − *Key Laboratory of Southwest China Wildlife Resources Conservation, College of Life Sciences, China West Normal University, Nanchong 637000, China; College of Environmental Science and Engineering, China West Normal University, Nanchong 637000, China*

Tongxu Liu − *Institute of Eco-Environmental and Soil Sciences, Guangdong Academy of Sciences, Guangzhou 510650, China;* orcid.org/0000-0002-2348-3952

Juan Liu − *The Key Laboratory of Water and Sediment Sciences, College of Environmental Sciences and Engineering, Peking University, Beijing 100871, China;* orcid.org/0000-0002-8456-203X

Zimeng Wang − *Department of Environmental Science and Engineering, Fudan University, Shanghai 200438, China;* orcid.org/0000-0002-4572-629X

Andreas Kappler − *Geomicrobiology Group, Department of Geosciences, University of Tübingen, Tübingen 72074, Germany;* orcid.org/0000-0002-3558-9500

Hailiang Dong − *Center for Geomicrobiology and Biogeochemistry Research, State Key Laboratory of Geomicrobiology and Environmental Change, China University of Geosciences, Beijing 100083, China; Frontiers Science Center for Deep-Time Digital Earth, China University of Geosciences, Beijing 100083, China;* orcid.org/0000-0002-7468-1350

Complete contact information is available at: https://pubs.acs.org/10.1021/acs.est.5c15463

Notes

The authors declare no competing financial interest.

ACKNOWLEDGMENTS

This project was supported by the National Natural Science Foundation of China (42577259, 42107278). We thank Prof. Yilin Hou and Ms. Jiayi He for their assistance with the microscopy experiments. We are also grateful to Dr. Yundang Wu for his valuable comments and suggestions during the revision of this manuscript, as well as to the anonymous reviewers for their constructive comments and helpful suggestions.

REFERENCES

(1) Hibbing, M. E.; Fuqua, C.; Parsek, M. R.; Peterson, S. B. Bacterial competition: surviving and thriving in the microbial jungle. *Nat. Rev. Microbiol.* **2010**, *8* (1), 15−25.

(2) Madigan, M.; Bender, K.; Buckley, D.; Sattley, W.; Stahl, D. *Brock Biology Of Microorganisms 15 Edn*. 2017.

(3) Andrews, S. C.; Robinson, A. K.; Rodríguez-Quiñones, F. Bacterial iron homeostasis. *Fems Microbiol. Rev.* **2003**, *27* (2−3), 215−237.

(4) Kappler, A.; Bryce, C.; Mansor, M.; Lueder, U.; Byrne, J. M.; Swanner, E. D. An evolving view on biogeochemical cycling of iron. *Nat. Rev. Microbiol.* **2021**, *19*, 360−374.

(5) Huang, J.; Jones, A.; Waite, T. D.; Chen, Y.; Huang, X.; Rosso, K. M.; Kappler, A.; Mansor, M.; Tratnyek, P. G.; Zhang, H. Fe(II) Redox Chemistry in the Environment. *Chem. Rev.* **2021**, *121* (13), 8161−8233.

(6) Dong, H.; Zeng, Q.; Sheng, Y.; Chen, C.; Yu, G.; Kappler, A. Coupled iron cycling and organic matter transformation across redox interfaces. *Nat. Rev. Earth Environ.* **2023**, *4*, 659−673.

(7) Raiswell, R.; Canfield, D. E. The iron biogeochemical cycle past and present. *Geochem. Perspect. Lett.* **2012**, *1*, 1−220.

(8) Melton, E. D.; Swanner, E. D.; Behrens, S.; Schmidt, C.; Kappler, A. The interplay of microbially mediated and abiotic reactions in the biogeochemical Fe cycle. *Nat. Rev. Microbiol.* **2014**, *12*, 797−808.

(9) McRose, D. L.; Newman, D. K. Redox-active antibiotics enhance phosphorus bioavailability. *Science* **2021**, *371* (6533), 1033−1037.

(10) Weber, K. A.; Achenbach, L. A.; Coates, J. D. Microorganisms pumping iron: anaerobic microbial iron oxidation and reduction. *Nat. Rev. Micro.* **2006**, *4* (10), 752−764.

(11) Bryce, C.; Blackwell, N.; Schmidt, C.; Otte, J.; Huang, Y.-M.; Kleindienst, S.; Tomaszewski, E.; Schad, M.; Warter, V.; Peng, C.; et al. Microbial anaerobic Fe(II) oxidation − Ecology, mechanisms and environmental implications. *Environ. Microbiol.* **2018**, *20* (10), 3462−3483.

(12) Klueglein, N.; Zeitvogel, F.; Stierhof, Y.-D.; Floetenmeyer, M.; Konhauser, K. O.; Kappler, A.; Obst, M. Potential role of nitrite for abiotic Fe(II) oxidation and cell encrustation during nitrate reduction by denitrifying bacteria. *Appl. Environ. Microbiol.* **2014**, *80* (3), 1051−1061.

(13) Dopffel, N.; Jamieson, J.; Bryce, C.; Joshi, P.; Mansor, M.; Siade, A.; Prommer, H.; Kappler, A. Temperature dependence of nitrate-reducing Fe(II) oxidation by Acidovorax strain BoFeN1 − evaluating the role of enzymatic vs. abiotic Fe(II) oxidation by nitrite. *FEMS Microbiol. Ecol.* **2021**, *11*, fiab155.

(14) Chen, D.; Cheng, K.; Liu, T.; Chen, G.; Kappler, A.; Li, X.; Zeng, R. J.; Yang, Y.; Yue, F.; Hu, S.; Cao, F.; Li, F. Novel insight into microbially mediated nitrate-reducing Fe(II) oxidation by *Acidovorax* sp. strain BoFeN1 using dual N−O isotope fractionation. *Environ. Sci. Technol.* **2023**, *57* (33), 12546−12555.

(15) Carlson, H. K.; Clark, I. C.; Blazewicz, S. J.; Iavarone, A. T.; Coates, J. D. Fe(II) oxidation is an innate capability of nitrate-reducing bacteria that involves abiotic and biotic reactions. *J. Bacteriol.* **2013**, *195* (14), 3260−3268.

(16) Pan, D.; Chen, P.; Yang, G.; Niu, R.; Bai, Y.; Cheng, K.; Huang, G.; Liu, T.; Li, X.; Li, F. Fe(II) Oxidation Shaped Functional Genes and Bacteria Involved in Denitrification and Dissimilatory Nitrate Reduction to Ammonium from Different Paddy Soils. *Environ. Sci. Technol.* **2023**, *57* (50), 21156−21167.

(17) Chen, D.; Liu, T.; Li, X.; Li, F.; Luo, X.; Wu, Y.; Wang, Y. Biological and chemical processes of microbially mediated nitrate-reducing Fe(II) oxidation by Pseudogulbenkiania sp. strain 2002. *Chem. Geol.* **2018**, *476*, 59−69.

(18) Giles, M. E.; Morley, N. J.; Baggs, E. M.; Daniell, T. J. Soil nitrate reducing processes − drivers, mechanisms for spatial variation, and significance for nitrous oxide production. *Front. Microbiol.* **2012**, *3*, 2012.

(19) Durand, S.; Guillier, M. Transcriptional and Post-transcriptional Control of the Nitrate Respiration in Bacteria. *Front. Mol. Biosci.* **2021**, *8*, 2021.
(20) Roothans, N.; van Loosdrecht, M. C. M.; Laureni, M. Metabolic labour division trade-offs in denitrifying microbiomes. *ISME J.* **2025**, *19*, wraf020.
(21) Kappler, A.; Schink, B.; Newman, D. K. Fe(III) mineral formation and cell encrustation by the nitrate-dependent Fe(II)-oxidizer strain BoFeN1. *Geobiology* **2005**, *3* (4), 235−245.
(22) Cheng, K.; Li, H.; Yuan, X.; Yin, Y.; Chen, D.; Wang, Y.; Li, X.; Chen, G.; Li, F.; Peng, C.; Wu, Y.; Liu, T. Hematite-promoted nitrate-reducing Fe(II) oxidation by Acidovorax sp. strain BoFeN1: Roles of mineral catalysis and cell encrustation. *Geobiology* **2022**, *20*, 810−822.
(23) Schmid, G.; Zeitvogel, F.; Hao, L.; Ingino, P.; Floetenmeyer, M.; Stierhof, Y.-D.; Schroeppel, B.; Burkhardt, C. J.; Kappler, A.; Obst, M. 3-D analysis of bacterial cell-(iron)mineral aggregates formed during Fe(II) oxidation by the nitrate-reducing Acidovorax sp. strain BoFeN1 using complementary microscopy tomography approaches. *Geobiology* **2014**, *12* (4), 340−361.
(24) Jiang, N.; Feng, Y.; Huang, Q.; Liu, X.; Guo, Y.; Yang, Z.; Peng, C.; Li, S.; Hao, L. Effect of Environmental pH on Mineralization of Anaerobic Iron-Oxidizing Bacteria. *Front. Microbiol.* **2022**, *13*, 885098.
(25) Liu, T.; Chen, D.; Li, X.; Li, F. Microbially mediated coupling of nitrate reduction and Fe(II) oxidation under anoxic conditions. *FEMS Microbiol. Ecol.* **2019**, *95* (4), fiz030.
(26) Kügler, S.; Cooper, R. E.; Wegner, C.-E.; Mohr, J. F.; Wichard, T.; Küsel, K. Iron-organic matter complexes accelerate microbial iron cycling in an iron-rich fen. *Sci. Total Environ.* **2019**, *646*, 972−988.
(27) Peng, C.; Shi, T.; Zhang, J.; Wu, Y.; Hu, S.; Liu, T.; Lu, L.; Kappler, A. Influence of bacterial strains and cell numbers on the reduction of Fe(III)-citrate and ferrihydrite with and without an electron shuttle. *ACS Earth Space Chem.* **2025**, *9* (2), 241−252.
(28) Joshi, P.; ThomasArrigo, L. K.; Sawwa, D.; Sauter, L.; Kappler, A. Complexation by Particulate Organic Matter Alters Iron Redox Behavior. *ACS Earth Space Chem.* **2024**, *8* (2), 310−322.
(29) Widdel, F.; Bak, F. Gram-Negative Mesophilic Sulfate-Reducing Bacteria. In *The Prokaryotes*; Springer: New York, NY, 1992; pp. 3352−3378.
(30) Stookey, L. L. Ferrozine—a new spectrophotometric reagent for iron. *Anal. Chem.* **1970**, *42* (7), 779−781.
(31) Klueglein, N.; Kappler, A. Abiotic oxidation of Fe(II) by reactive nitrogen species in cultures of the nitrate-reducing Fe(II) oxidizer *Acidovorax* sp. BoFeN1 − questioning the existence of enzymatic Fe(II) oxidation. *Geobiology* **2013**, *11* (2), 180−190.
(32) Pierce, J.; Suelter, C. An evaluation of the Coomassie brilliant blue G-250 dye-binding method for quantitative protein determination. *Anal. Biochem.* **1977**, *81* (2), 478−480.
(33) Jiao, Y.; Kappler, A.; Croal, L. R.; Newman, D. K. Isolation and characterization of a genetically tractable photoautotrophic Fe(II)-oxidizing bacterium, *Rhodopseudomonas palustris* strain TIE-1. *Appl. Environ. Microb.* **2005**, *71* (8), 4487−4496.
(34) Schwertmann, U.; Cornell, R. M.. *Iron oxides in the laboratory: preparation and characterization*; John Wiley & Sons, 2008.
(35) Chen, R.; Liu, H.; Tong, M.; Zhao, L.; Zhang, P.; Liu, D.; Yuan, S. Impact of Fe(II) oxidation in the presence of iron-reducing bacteria on subsequent Fe(III) bio-reduction. *Sci. Total Environ.* **2018**, *639*, 1007−1014.
(36) Miot, J.; Benzerara, K.; Morin, G.; Kappler, A.; Bernard, S.; Obst, M.; Férard, C.; Skouri-Panet, F.; Guigner, J.-M.; Posth, N.; Galvez, M.; Brown, G. E.; Guyot, F. Iron biomineralization by anaerobic neutrophilic iron-oxidizing bacteria. *Geochim. Cosmochim. Acta* **2009**, *73* (3), 696−711.
(37) Schädler, S.; Burkhardt, C.; Hegler, F.; Straub, K. L.; Miot, J.; Benzerara, K.; Kappler, A. Formation of cell-iron-mineral aggregates by phototrophic and nitrate-reducing anaerobic Fe(II)-oxidizing bacteria. *Geomicrobiol. J.* **2009**, *26* (2), 93−103.
(38) Larese-Casanova, P.; Haderlein, S. B.; Kappler, A. Biomineralization of lepidocrocite and goethite by nitrate-reducing Fe(II)-oxidizing bacteria: Effect of pH, bicarbonate, phosphate, and humic acids. *Geochim. Cosmochim. Acta* **2010**, *74* (13), 3721−3734.
(39) Zhao, L.; Dong, H.; Kukkadapu, R.; Agrawal, A.; Liu, D.; Zhang, J.; Edelmann, R. E. Biological oxidation of Fe(II) in reduced nontronite coupled with nitrate reduction by Pseudogulbenkiania sp. Strain 2002. *Geochim. Cosmochim. Acta* **2013**, *119*, 231−247.
(40) Huang, G.; Wang, X.; Pan, D.; Yang, G.; Zhong, R.; Niu, R.; Xia, B.; Cheng, K.; Liu, T.; Li, X. Cadmium immobilization during nitrate-reducing Fe(II) oxidation by Acidovorax sp. BoFeN1: Contribution of bacterial cells and secondary minerals. *Chem. Geol.* **2023**, *639*, 121729.
(41) Miot, J.; Remusat, L.; Duprat, E.; Gonzalez, A.; Pont, S.; Poinsot, M. Fe biomineralization mirrors individual metabolic activity in a nitrate-dependent Fe(II)-oxidizer. *Front Microbiol.* **2015**, *6*, 879.
(42) Maia, L. B.; Moura, J. J. G. How Biology Handles Nitrite. *Chem. Rev.* **2014**, *114* (10), 5273−5357.
(43) Klar, J. K.; Homoky, W. B.; Statham, P. J.; Birchill, A. J.; Harris, E. L.; Woodward, E. M. S.; Silburn, B.; Cooper, M. J.; James, R. H.; Connelly, D. P.; Chever, F.; Lichtschlag, A.; Graves, C. Stability of dissolved and soluble Fe(II) in shelf sediment pore waters and release to an oxic water column. *Biogeochemistry* **2017**, *135* (1), 49−67.
(44) Pierri, D.; Czop, M. Iron index as an organic matter decay intensity indicator in a shallow groundwater system highly contaminated with phenol (case study in northern Poland). *Environ. Earth Sci.* **2020**, *79* (12), 287.
(45) Ho, T.-Y.; Taylor, G. T.; Astor, Y.; Varela, R.; Müller-Karger, F.; Scranton, M. I. Vertical and temporal variability of redox zonation in the water column of the Cariaco Basin: implications for organic carbon oxidation pathways. *Mar. Chem.* **2004**, *86* (1), 89−104.
(46) Catrouillet, C.; Davranche, M.; Dia, A.; Bouhnik-Le Coz, M.; Marsac, R.; Pourret, O.; Gruau, G. Geochemical modeling of Fe(II) binding to humic and fulvic acids. *Chem. Geol.* **2014**, *372*, 109−118.
(47) Sundman, A.; Karlsson, T.; Persson, P. An experimental protocol for structural characterization of Fe in dilute natural waters. *Environ. Sci. Technol.* **2013**, *47* (15), 8557−8564.
(48) Li, H.; Cheng, K.; Zhang, Y.; Li, X.; Zhu, X.; Wu, Y.; Chen, G.; Yang, Y.; Guo, C.; Liu, T. Biogenic iron minerals as a potential survival mechanism for nitrate-reducing iron-oxidizing bacteria. *Geochim. Cosmochim. Acta* **2025**, *397*, 53−62.
(49) Geelhoed, J. S.; Hiemstra, T.; Van Riemsdijk, W. H. Competitive Interaction between Phosphate and Citrate on Goethite. *Environ. Sci. Technol.* **1998**, *32* (14), 2119−2123.
(50) Weber, K. A.; Pollock, J.; Cole, K. A.; O'Connor, S. M.; Achenbach, L. A.; Coates, J. D. Anaerobic nitrate-dependent iron(II) bio-oxidation by a novel lithoautotrophic betaproteobacterium, strain 2002. *Appl. Environ. Microb.* **2006**, *72* (1), 686−694.
(51) Chen, G.; Chen, D.; Li, F.; Liu, T.; Zhao, Z.; Cao, F. Dual nitrogen-oxygen isotopic analysis and kinetic model for enzymatic nitrate reduction coupled with Fe(II) oxidation by Pseudogulbenkiania sp. strain 2002. *Chem. Geol.* **2020**, *534*, 119456.
(52) Xiu, W.; Guo, H.; Shen, J.; Liu, S.; Ding, S.; Hou, W.; Ma, J.; Dong, H. Stimulation of Fe(II) Oxidation, Biogenic Lepidocrocite Formation, and Arsenic Immobilization by Pseudogulbenkiania Sp. Strain 2002. *Environ. Sci. Technol.* **2016**, *50* (12), 6449−6458.

https://doi.org/10.1021/acs.est.5c15463
Environ. Sci. Technol. 2026, 60, 8507−8516